

THE DESIGN AND CONSTRUCTION OF A POWERFUL ELECTROMAGNET,
AND ITS APPLICATION TO MAGNETIC MEASUREMENTS OF THE ALLOY $\text{Mn}_{60}\text{Al}_{20}\text{C}_{20}$.

by

GEOFFREY VICTOR KIDSON.

A THESIS SUBMITTED IN PARTIAL FULFILMENT OF
THE REQUIREMENTS FOR THE DEGREE OF

MASTER OF SCIENCE

in the Departments

of

Physics and Metallurgy

We accept this thesis as conforming to the standard required from candidates
for the degree of MASTER OF SCIENCE.

Members of the Departments
of Physics and Metallurgy.

THE UNIVERSITY OF BRITISH COLUMBIA

OCTOBER 1953.

SYNOPSIS.

An electromagnet capable of producing a magnetic field intensity of greater than 21,600 gauss in a gap of one inch and over an area of 3.14 square inches has been designed and constructed.

The structure of the ternary alloy of approximate composition $\text{Mn}_{60}\text{Al}_{20}\text{C}_{20}$ has been investigated by X-ray methods, and shown to have an ordered perovskite structure, with $a_0 = 3.865 \text{ \AA}$.

The effective magnetic moment per manganese atom was measured, using the electromagnet, and a torsion balance method. The value of the magnetic moment at zero degrees Kelvin was found to be 1.2 Bohr magnetons per manganese atom.

ACKNOWLEDGEMENT

The author is grateful for financial aid in the form of a National Research Council Bursary during the winter of 1952-53, and the summer of 1953. Without such aid this work could not have been carried out.

Mr. F. K. Bowers, of the Physics department made many valuable suggestions concerning the design of the magnet.

The funds for the construction of the electromagnet were provided by the Defense Research Board.

The iron for the yoke of the magnet was donated through the generosity of the Steel Co. of Canada, Hamilton.

The author is grateful to members of the staff of the Department of Mining and Metallurgy for helpful technical advice.

TABLE OF CONTENTS

	page
TITLE PAGE	i
TABLE OF CONTENTS.	ii
INDEX OF ILLUSTRATIONS AND TABLES.	iii
SYNOPSIS	iv
ACKNOWLEDGEMENT.	v
<u>PART 1:</u> 'THE DESIGN, CONSTRUCTION AND PERFORMANCE OF THE ELECTROMAGNET'	
INTRODUCTION	1
PREVIOUS WORK.	5
TESTING OF SCHNAY MAGNET	7
THE DESIGN OF THE ELECTROMAGNET.	10
THE CONSTRUCTION AND ASSEMBLY OF THE MAGNET.	15
PERFORMANCE OF THE MAGNET.	17
DISCUSSION.	18
<u>PART 2:</u> 'AN INVESTIGATION OF THE MANGANESE - RICH FERROMAGNETIC ALLOY OF APPROXIMATE COMPOSITION $Mn_{60}Al_{20}C_{20}$.'	
INTRODUCTION	24
PREVIOUS WORK.	28
PROCEDURE.	29
RESULTS.	32
DISCUSSION AND CONCLUSIONS	37
APPENDIX I.	43
APPENDIX II	47

ILLUSTRATIONS AND TABLES

	Figure No.	Plate No.
Schnay Magnet.....	1	I
Final Design of New Magnet.....	2	II
Wiring Diagram of Coils.....	3	III
Components of Coil Assembly.....	4	IV
Completed Magnet.....	5,6	V, VI
Field vs. Current.....	7	VII
Apparatus for Resistance Measurements.....	8	VIII
Magnetic Moments vs. Electrons per Atom.....	9	IX
Debye-Sherrer X-ray Patterns.....	10	X
Pole Piece Design.....	11	XI

	Table No.	Page No.
Measurements of Magnetic Moments on Schnay Magnet.....	1	8
Ratio of Interatomic Distance to Radius of 3d Shell	2	26
Heat Treatments of Alloy.....	4	32
Analyses of Samples.....	5	33
Magnetic Measurements.....	6	35
Intensity Measurements.....	7	35
Structure Factor Calculations.....	8	39

PART 1.

THE DESIGN, CONSTRUCTION, AND PERFORMANCE OF THE ELECTROMAGNET

Introduction

Magnetism is a universal property of matter. All substances respond to magnetic influence to a greater or lesser extent when placed in a strong magnetic field of force, as near to a pole of an electromagnet.

From the standpoint of magnetic susceptibility there are three general classes of substances:

- (a) Substances that are repelled by a magnetic pole are called diamagnetic.
- (b) Substances that are weakly attracted by a magnetic pole are called paramagnetic.
- (c) Substances that are relatively very strongly attracted by a magnetic pole are called ferromagnetic.

In addition to the elements Fe, Co, Ni, there are many alloys which are classified as ferromagnetic substances. For the present, it may be assumed that within a ferromagnetic substance there are innumerable elementary magnet dipoles associated with the atoms or the molecules of the substance. Present theories regarding the nature of these elementary dipoles will be considered later.

If the substance is placed in a magnetic field of force, the elementary dipoles will tend to align themselves in the direction of the external field, thus causing the atoms to become polarized. Within the substance, the negative side of one atom faces the positive side of the next atom, and the elementary dipoles will cancel one another. At the ends however, there will be free poles and the bar as a whole will be polarized. If the surface densities of polarization at the ends are $+s$ and $-s$, the magnetic moment of the bar as a whole is sAl , where A = cross sectional area and l = length. Then the magnetic moment per unit volume = $\frac{sAl}{Al} = s$.

This quantity is usually denoted by M . If a measure of the magnetic moment per unit volume can be obtained, then knowing the number of atoms per unit volume, the magnetic moment per atom can be determined. The latter is an important experimental quantity and is useful in any attempt to describe the ultimate nature of the elementary dipoles within the atoms.

One of the methods of determining M is by measuring the force F_x exerted on the sample of the ferromagnetic substance when it is placed in a magnetic field H . It can be shown that this force is given by

$$F_x = KM \frac{\partial H}{\partial x}$$

where K is a constant of proportionality, and $\frac{\partial H}{\partial x}$ is the gradient of the field in the x -direction.

If the field is designed such that $\frac{\partial H}{\partial x} = \text{constant}$, and $\frac{\partial H}{\partial y} = \frac{\partial H}{\partial z} = 0$, then we have

$$F_x = \vec{F} \propto M$$

Thus the requirements for a field suitable for making measurements of M by

measuring the force on the sample are simply

- (a) That $\frac{\partial H}{\partial x}$ be constant over the sample

where $\frac{\partial H}{\partial y} = \frac{\partial H}{\partial z} = 0$. and

- (b) That the external applied field H be sufficiently strong so as to align all the elementary dipoles, thereby giving a true measure of M . Such a condition is known as saturation.

The first of these requirements can be met by suitable shaping of the pole pieces of the magnet. A simple and accurate method of measuring the force on the sample is that of the torsion balance. That is, by arranging that the angle of twist of a fine wire suspension required to return the sample to its initial position in the field, before the field was on, be proportional to the force exerted on the sample, we have a direct proportionality between the angle of twist of the suspension and the magnetic moment of the sample.

If comparison is then made to a standard sample whose magnetic moment is known, the moment of the unknown sample may readily be determined.

The fulfillment of requirement (b) is hindered by what is known as the demagnetizing effect. This arises from the field produced by the free poles of the magnetic substance itself and extends throughout the sample in opposite direction to the applied external field, thereby acting to reduce the effective applied field. The effect is dependent upon the geometry of the sample measured. The resultant field within the bar can be expressed as:

$$H_i = H_e - NM_s$$

where N = demagnetizing factor,

H_i = resultant internal field,

H_e = external field.

The resultant field for a spherical specimen, for example, can be as small as 0.003 of the external field. Thus in order that saturation be produced in powdered samples, large fields must be used.

PREVIOUS WORK

A small electromagnet, whose design was adopted from that of Buehl and Wulff¹, has been built and used in the department by Schnay². Originally it was intended for use in studies of phase transformations in ferrous alloys.

The pole pieces were designed so as to produce a constant field gradient along the axis of the pole pieces. The force exerted on a sample was found by means of a torsion balance; the angle of twist required to bring the sample back to its original position in the field being proportional to the force.

Piercy³ investigated the characteristics of the magnet, and found them satisfactory for carrying out measurements of magnetic moment for cylindrically shaped specimens whose ratio of diameter to length was 1:5.

The Schnay magnet is shown in figure 1, Plate I.

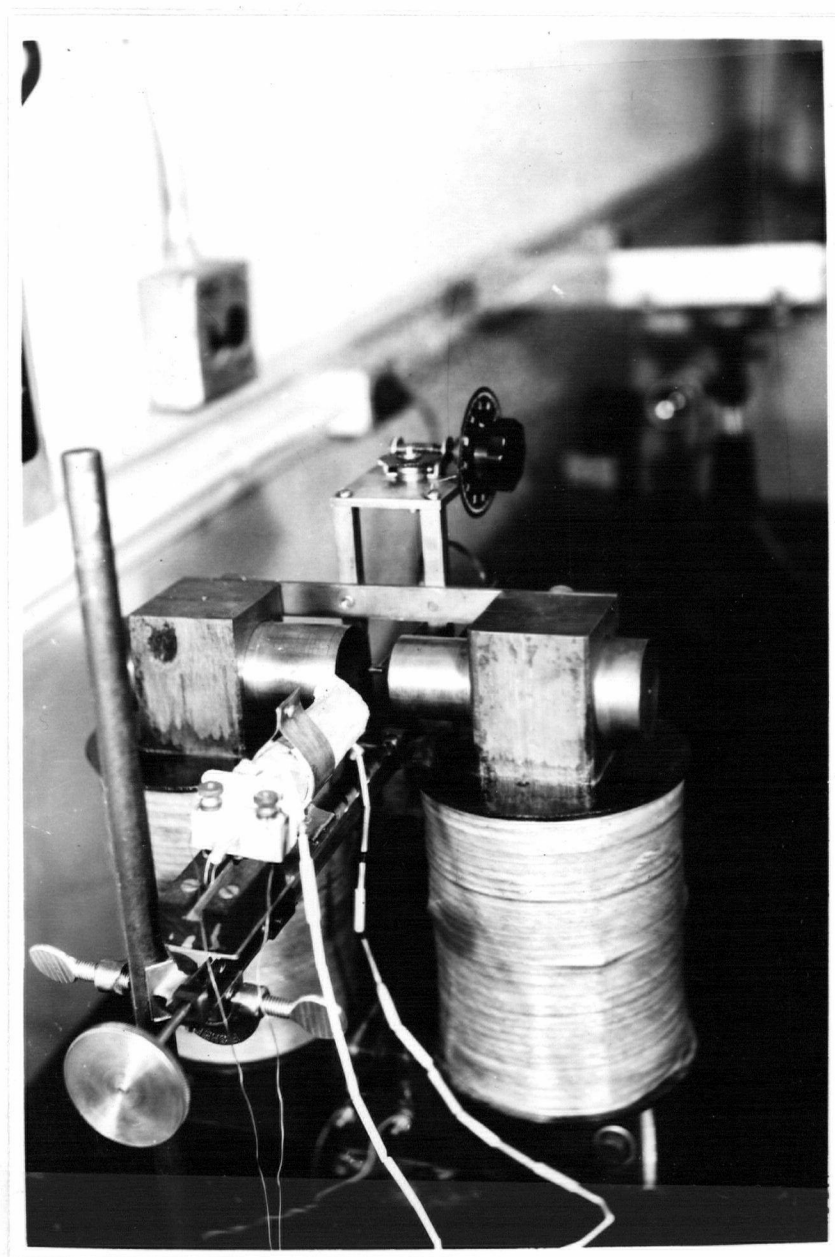


Figure 1. Schnay magnet, showing the furnace used for
Curie temperature determinations.

TESTING OF THE SCHNAY MAGNET

The Schnay magnetic balance appeared capable of fulfilling the requirements described on page 3, for carrying out measurements of the magnetic moments of solid cylindrical specimens³, however it was not known if saturation could be produced in powdered samples.

Many of the alloys under investigation were extremely brittle, and it was impossible to obtain samples in cylindrical form. Either irregular shapes or powdered samples had to be used.

It was decided, therefore, that an investigation of the Schnay magnet be made, using powdered samples of standard iron and nickel, to determine if the samples were saturated.

A wide range of particle sizes was obtained by using screen meshes. The finely divided metal was mixed with a solution of guncotton dissolved in butyl acetate. Cylindrical samples were formed by an extrusion method. The butyl acetate evaporated leaving a strong sample of the powdered metal bonded by the guncotton.

The results of the measurements are shown in Table 1. It can be seen that the agreement between the solid and powdered samples is poor. The smallest difference occurring is 4%.

TABLE 1.

Screen Size	$\Delta \theta$ /mg. for Ni	$\Delta \theta$ /mg. for Fe
Solid sample	1.616	
80-200 mesh.	1.520	4.720
200-270 "	1.525	4.690
270-325 "	1.550	4.600
-325 "	1.552	4.630

Attempts were made to improve the measurements by modifying the magnetic balance. The small bucket used to hold the sample was found to give an appreciable deflection when no sample was in it. Piercy had allowed for this by correcting his angle of twist. However it was found that the amount of deflection due to the bucket was not constant.

Suitable substitute materials were tested by suspending them by a fine thread in the field, and observing the resultant deflection when the field was applied. A rod of commercial silver solder was thus found to be very nearly unaffected. A new sample holder using a copper bucket and solder arm was made up and used.

An instability of the field near the center of the gap was noted. This made consistent zero point readings difficult. It was assumed that the instability of the field was inherent in the design of the magnet, since any leakage flux from the coils was perpendicular to the flux between the pole pieces, causing a distortion of the field. Steel plates were placed around the ends of the coils in an attempt to decrease the leakage flux. Although the shields were successful in improving the stability of the readings, the discrepancies between the solid and powder-

ed samples remained.

Fluctuations of current in the coils due to resistance changes with heating, were eliminated by including a small rheostat in the circuit for fine adjustments of current.

It was concluded that the large discrepancies in readings for the different particle sizes were primarily due to the samples not reaching saturation. Two methods were used in attempts to increase the field strength in the gap. By connecting the coils in parallel, the current was increased from 4.0 amperes to a maximum of 8.0 amperes. The field strength was measured with a flux meter and search coil. The maximum field obtained in this way was only 3000 gauss.

The notable lack of increase of the field strength in proportion to the increase in current, and hence in total ampere - terms, was thought to be due to the poor placement of the coils. This resulted in the yoke of the magnet becoming saturated whereas the pole pieces were not. The effect of this upon the field strength in the gap will be more fully discussed on page 13.

Ewing⁴ has shown that the optimum shape of pole piece to produce a maximum field is a cone, with an angle of taper of $54^{\circ} 44'$. Pole pieces were made up and the field strength measured, using various gap widths and currents. The largest value of the field obtained in this way was 7000 gauss, using a gap of $3/8"$ and a current of 8 amps.

Since Sucksmith⁵ reported being unable to produce saturation of powdered samples in fields as high as 16000 gauss, it was decided that a more powerful electromagnet must be constructed for the magnetic measurements of the new alloy systems.

THE DESIGN OF THE ELECTROMAGNET

A starting point in the design problem of the electromagnet was provided by certain requirements that had to be fulfilled.

In order that the powdered samples be saturated, a field strength of at least 18000 gauss was chosen. The gap between the pole pieces had to be of sufficient size to permit measurements to be made at room temperature, and also using a dewar flask for low temperatures. The one inch gap used in the Schnay magnet was considered satisfactory, and this value was adopted for the new magnet.

Further considerations involved the available electrical power, the dissipation of heat from the coils and the availability of materials. Finally, of course, consideration had to be given to the overall cost of the materials and construction.

The details of the calculations are given in Appendix 1, however the general scheme used will be outlined here.

In the magnetic circuit, the energy required to produce the magnetic flux is provided by the magnetomotive force. The latter, in turn, is provided by the ampere-turns in the circuit, i.e. the product of the number of amperes times the number of turns in the coils.

An approximate determination of the total ampere-turns required can be obtained from the relation:

$$NI = \oint H dl = H_a l_a + H_i l_i.$$

where

N = number of turns

H_i = field strength in iron

I = current

l_a = path length in air

H_a = field strength in air

l_i = path length in iron

A major portion of the magnetomotive force will be dropped across the air gap, hence a first approximation of the total ampere-turns required can be obtained using

$$(NI - H_1 l_1) = H_a l_a.$$

From this calculation, and many trial and error designs, it was estimated that the total number of ampere turns required was 45,000.

Since the yoke had to be large enough to accomodate the coils, the latter were considered first.

The method of dissipating the heat from the coils was one adopted from a number of alternatives. From considerations of the total size of the coil assembly, and the efficiency of cooling, a system of water cooling pancakes interspersed between the coils was chosen as that best suited to the requirements, and contributing to the most economical design.

The size and shape of the coil assemblies were determined by the power which could be dissipated in them, which in turn was determined by the rate of flow of water through the cooling pancakes. Assuming an allowable temperature rise of 20°C, and a rate of flow of water of 50 cc/sec., the power to be dissipated was found to be 4180 watts. From this figure and the estimated number of ampere-turns required, the effective parallel resistance of all turns was determined.

It was decided that the cooling pancakes were to be of such a size that one-third of the total cross-sectional area of the coils was copper. The remainder of the space would be taken up by the cooling pancakes, insulation and the packing factor of the wire in the coils. Empirical values of the packing factor for various wire sizes were obtained from Roters⁶.

This choice of area allotted to the copper wire determined the ratio of the mean-turn length to total cross-sectional area of the coil assembly, as outlined in Appendix 1.

The values of mean-turn length, cross sectional area, and the final dimensions of the coils were then found from the size of the pole piece. Considerations determining the choice of the shape and size of the pole piece are discussed below.

The choice of the wire size was determined by the voltage of the source. At the time of the design of the magnet, the d.c. source had not been decided upon, hence a source giving 120 volts was assumed. Using this value, the closest commercial wire size was #10 wire. Square wire was chosen for its superior packing factor.

Using #10 wire, the following specifications were determined:

Number of turns	1292
Current	34.8 amps.
Resistance of coils (series)	3.42 ohms.
Voltage required	119.2 volts.
Power to be dissipated	4150 watts.

One of the main difficulties encountered in the magnetic circuit calculations is that of the flux leakage. Not all of the flux from the pole pieces will be concentrated within the gap, but will tend to be spread out over a considerably larger area, resulting in a diminution of the field strength in the gap. It is therefore necessary to make the cross-sectional area of the pole piece face large enough to insure that a reasonably uniform field intensity will exist over the sample, perpendicular to the axis of the pole pieces and that this field intensity be sufficient to produce saturation in the sample.

The effect of the leakage factor can be nullified by making use of a geometrical factor. That is, if the pole pieces are tapered so that the ratio of the area of the large end to that of the small end is equal to the leakage factor, then the geometrical factor will tend to increase the flux density in opposition to the loss due to leakage. In this way, the flux density in the iron of the pole piece is known to be required to be 18000 gauss, since this is the value chosen for the gap field strength.

On calculating the leakage factor of the pole pieces, the following assumptions were made:

- (a) All flux falling outside the arc of a circle whose center is at the gap center, and whose radius is equal to the distance from the gap center to the shoulder of the pole piece, can be neglected.
- (b) It is assumed that the field intensity across the gap is constant, and that it falls off as $\frac{1}{r}$ outside the gap, where r is the distance from the axis of the pole pieces.

Using these assumptions, the leakage factor was found to be 9.

It was pointed out on page 9, that one of the faults in the design of the Schnay magnet was that the yoke became saturated before the pole pieces did. In the magnetic circuit, the amount of magnetomotive force 'dropped' across a given component will depend upon the reluctance of that component. It is desirable to have the maximum amount possible of the magnetomotive force produced by the coils to be dropped across the air gap. Thus the reluctance of the yoke should be kept small. The reluctance increases in the iron as saturation is approached. In order to avoid saturation the flux density should be kept small, and this can be

done by using a large cross-sectional area in the yoke.

The placement of one coil assembly on each pole piece gave further assurance that the pole pieces would be saturated before the yoke.

As was discussed on page 3, it is desirable, for the purpose of measuring the magnetic moment of the samples by the 'torsion balance' method, to have a constant field gradient along the axis of the pole pieces, and zero field gradient perpendicular to the axis.

In the design of a non-uniform field, having special characteristics, Fereday⁷ pointed out that the flux lines can be assumed to leave and enter the pole pieces normal to the surfaces of the pole pieces. On the basis of this assumption, it was proposed that a field gradient of the desired characteristics could be produced by having one concave pole face and one convex, the two having a common center of curvature. The magnitude of the gradient, and hence the force exerted on the sample could be controlled by choosing a suitable ratio of poleface area.

It was anticipated that the actual characteristics of the field would not follow the ideal case as discussed above. Hence the pole pieces were designed to have removable caps to facilitate a change of the shape of the pole cap if necessary.

The final design is shown in Figure 2, Plate II.

THE CONSTRUCTION AND ASSEMBLY OF THE MAGNET.

The coils were wound into pancakes, each pancake consisting of three layers of double cotton covered wire. The wires were coated with air-drying glyptal varnish, and wound on wooden bobbins, which were removed when the varnish was dry, leaving the coils self-supporting.

The water cooling pancakes were made of two copper pans, one fitted inside the other. An internal spiral of copper strip forced the cooling water to follow a circuitous path in the pancake, insuring good circulation.

The coils and cooling pancakes were made up into two assemblies. Each assembly consisted of four coils and five cooling pancakes. An insulating sheet of drawing paper coated with glyptal varnish separated the coils from the cooling pancakes. The coil assemblies were fitted on to the pole pieces by using wooden rings, tapered on the inside to fit the pole piece and flat on the outside to fit the coil or cooling pancake. Matching slots in the wooden rings permitted the wires from the inside of the coils to be brought out along the surface of the pole piece. This facilitated the making of connections between the coils.

A diagram of the wiring of the coils is shown in Figure 3, Plate III.

In order to prevent the cooling pancakes from bursting due to the large force exerted over their surface, the completed assembly was placed between two 5/8 inch brass plates, which were bolted together.

The pole pieces were secured to the yoke by a large bolt, passed through the yoke and screwed into the pole piece. Figure 4, Plate IV shows the components of one coil assembly.

Originally the yoke was to be 6 inches square, however the only available iron suitable for the magnet was 4 1/2" x 8". It was necessary to have the iron forged to 6" x 6" at the top of the yoke to accomodate the 6" diameter pole pieces. The forging of the yoke was done by the B.C. Marine Company.

The inside faces of the yoke were machined at the Sumner Iron Works.

The pole pieces were machined by Mr. R. Richter in the Metallurgy shop. Special high purity iron was used for the pole caps.

The assembled magnet was put on a portable base.

Both hot and cold water could be mixed in the cooling system so as to provide any initial temperature of cooling water desired. By this means, excessive condensation on the brass plates was avoided. The water was connected in parallel in the cooling system, by using a common manifold. A pressure gauge was installed in the water line. It was found that an operating pressure of 3-5 p.s.i. was adequate.

The direct current was supplied by a Hobart Welding generator. This generator was chosen in preference to others because of its small a.-c. ripple, remote control rheostat and low cost. It is capable of giving a current range of 0 to 200 amperes at a voltage of 40 volts. The coils were connected in parallel to operate at low voltage and high current. Figure 5, Plate V shows the completed magnet with the torsion balance.

PLATE II

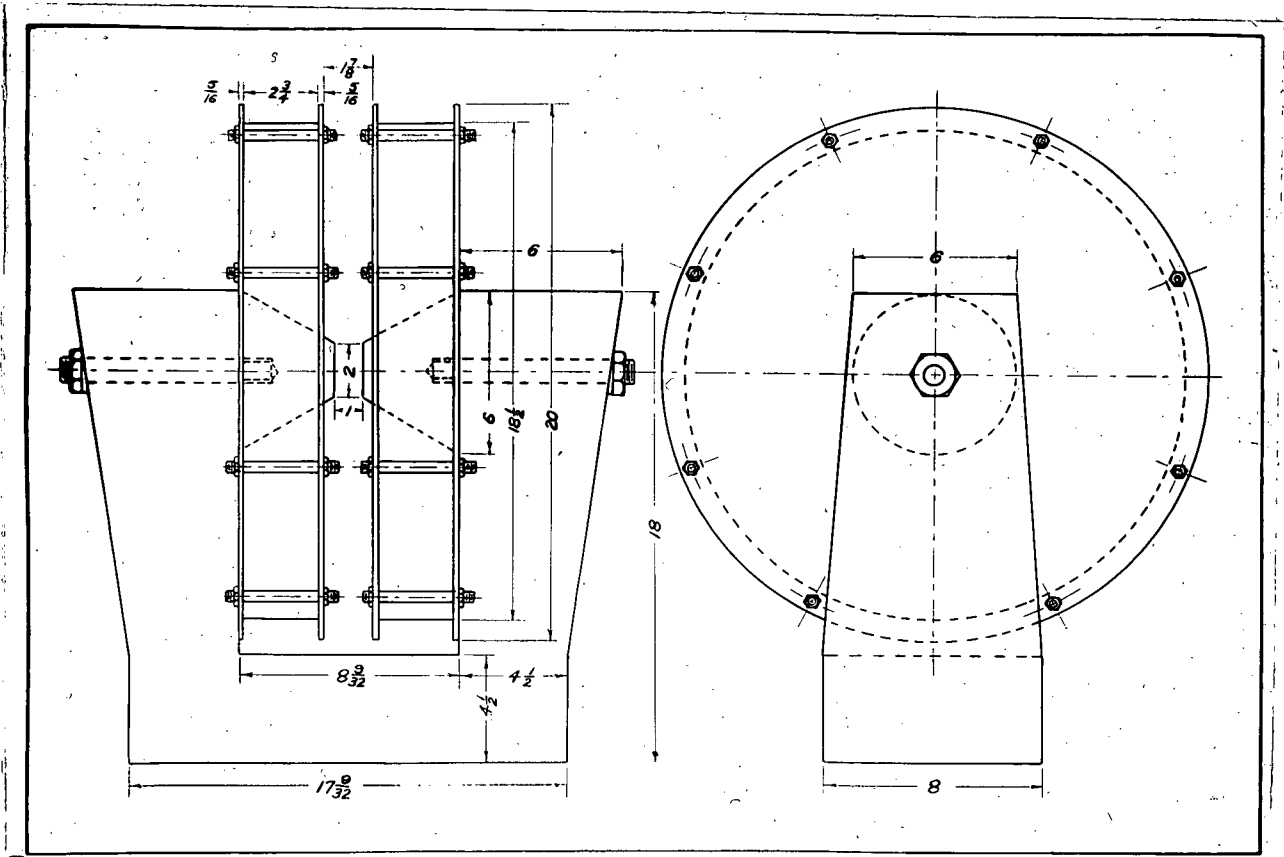


Figure 2. The Final design of the new magnet.

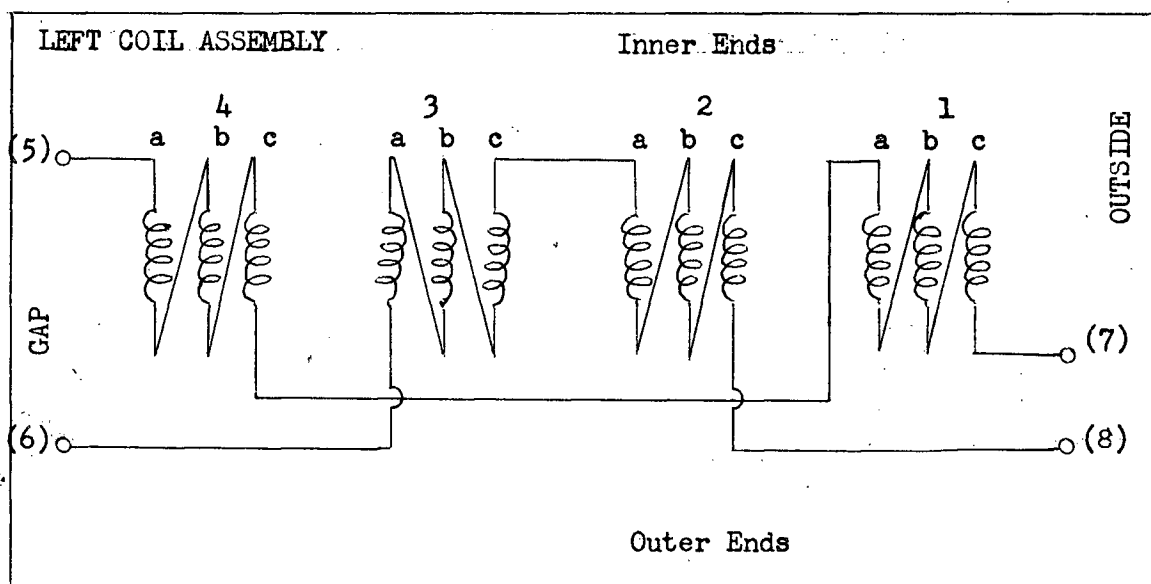
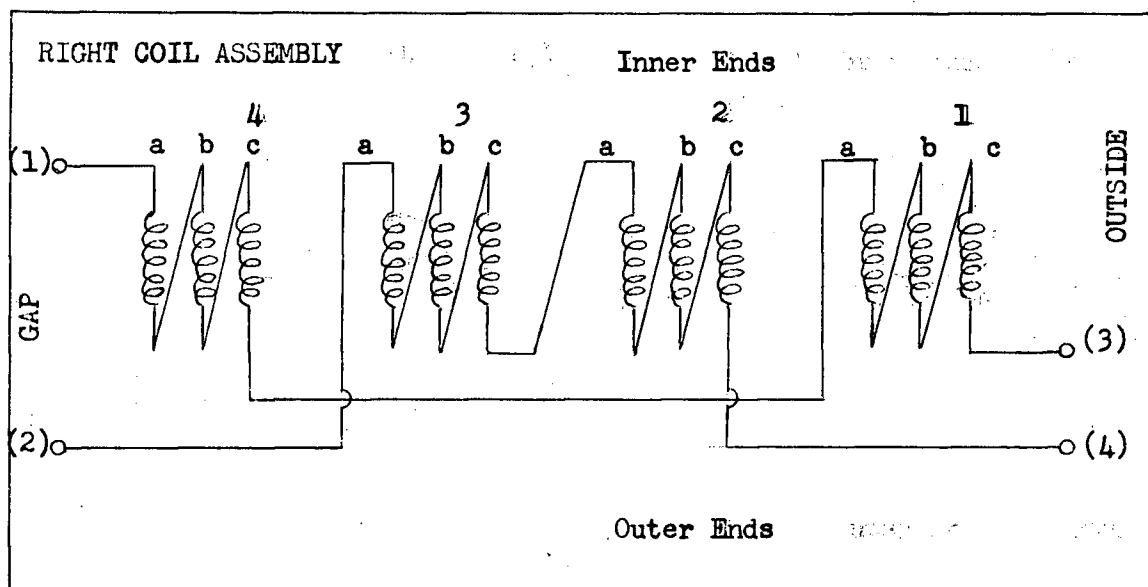


Figure 3. Wiring Diagram of Coils

Coils 1, 2, 3, 4 (right) and coil 3 (left) are wound in the same direction. Coils 1, 2, 4 (left) are wound in the opposite direction to these. The diagram of each coil assembly shows the coils in the physical order in which they are assembled on the magnet.

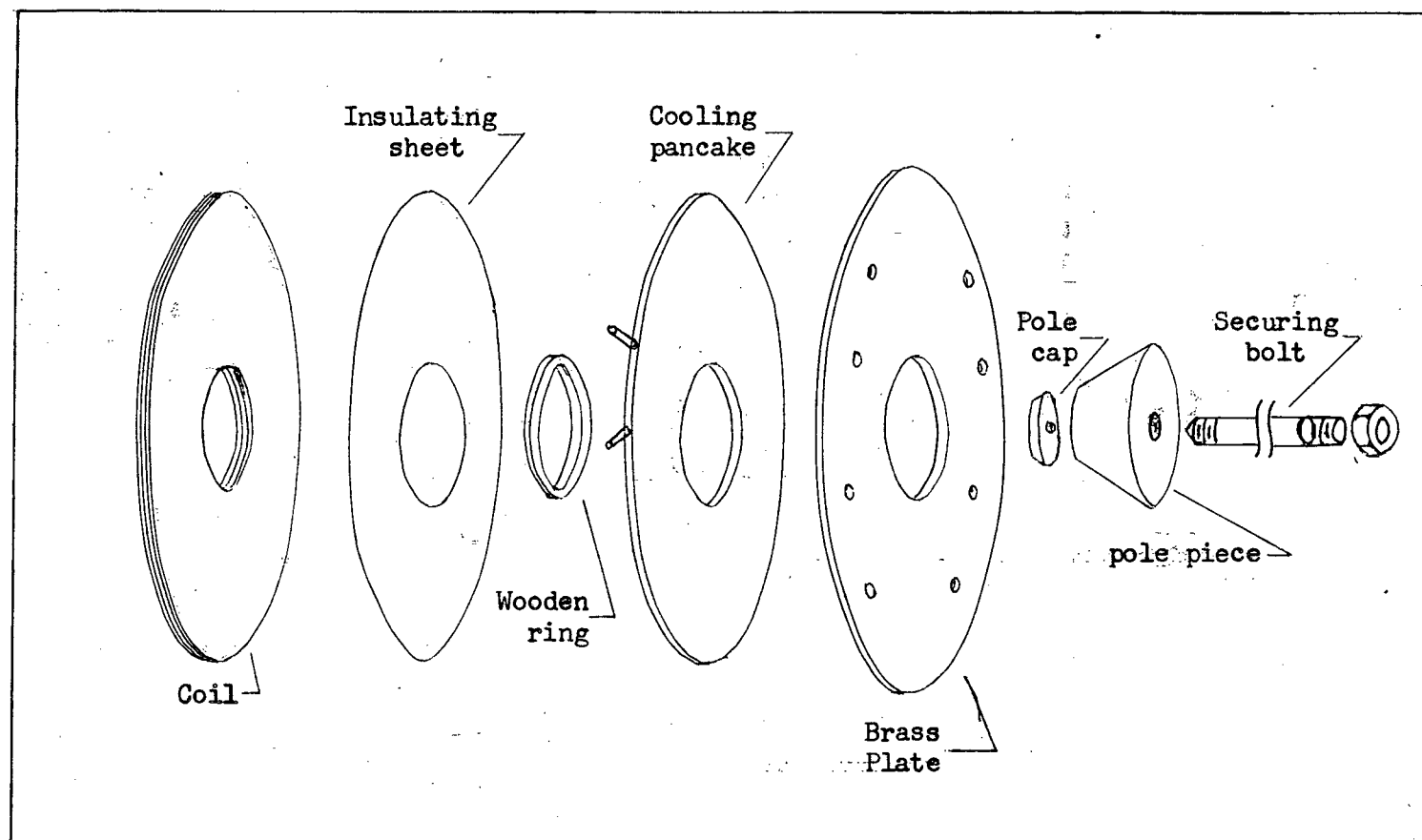


Figure 4. Component parts of one coil assembly are shown. See page 15 for full description of the coil assemblies.

PERFORMANCE OF THE ELECTROMAGNET.

A preliminary test of the rate of flow of water in the pancakes was made by enclosing the pancakes in two heavy plywood boards, which were bolted together. Using the pressure directly from the tap, a flow of 50 c.c./sec. was easily obtained, and up to 200 c.c./sec. was possible.

The coils and cooling pancakes were assembled, using a dummy wooden pole piece. The cooling of the coils was tested by taking the readings of voltage across and the current through the coils. From this the resistance changes, and hence the temperature changes were plotted against time. Runs were continued for periods of one hour, at currents up to 50 amperes.

The maximum temperature rise was only 9°C . Thus the coils were found capable of taking large currents, producing up to 65,000 ampere turns.

The field strength of the magnet was measured with a flux meter and search coil, borrowed from the Physics department. These had been calibrated using a proton resonance method. The maximum field strength measured, using a current of 52.5 amperes and flat pole caps was 21,500 gauss.

The field strength in the center of the gap is plotted against the current in Figure 7, Plate VII.

DISCUSSION.

The work thus far described was carried out jointly by Mr. R. M. Shier, and the author.

The remainder of the work, namely the production of a constant field gradient along the axis of the pole pieces, and the design and construction of the torsion balance, was carried out independently by Mr. Shier⁸.

The rather large field strength obtained indicated that the magnet would be capable of producing saturation in the powdered samples. Subsequent work verified this to be so.

When the cooling pancakes were first tested, they were lying horizontally. It was observed that in the assembled position, in which the pancakes were vertical, the top of the coils became quite warm. This was attributed to air being trapped in the cooling pancakes, preventing water from circulating properly, and dissipating the heat.

To overcome this difficulty, small holes were drilled in the tops of the cooling pancakes. This permitted the air to escape. The pancakes were filled with water, the holes were tapped, and sealed using small screws, a rubber gasket and sealing cement. Prolonged running of the magnet produced no further heating.

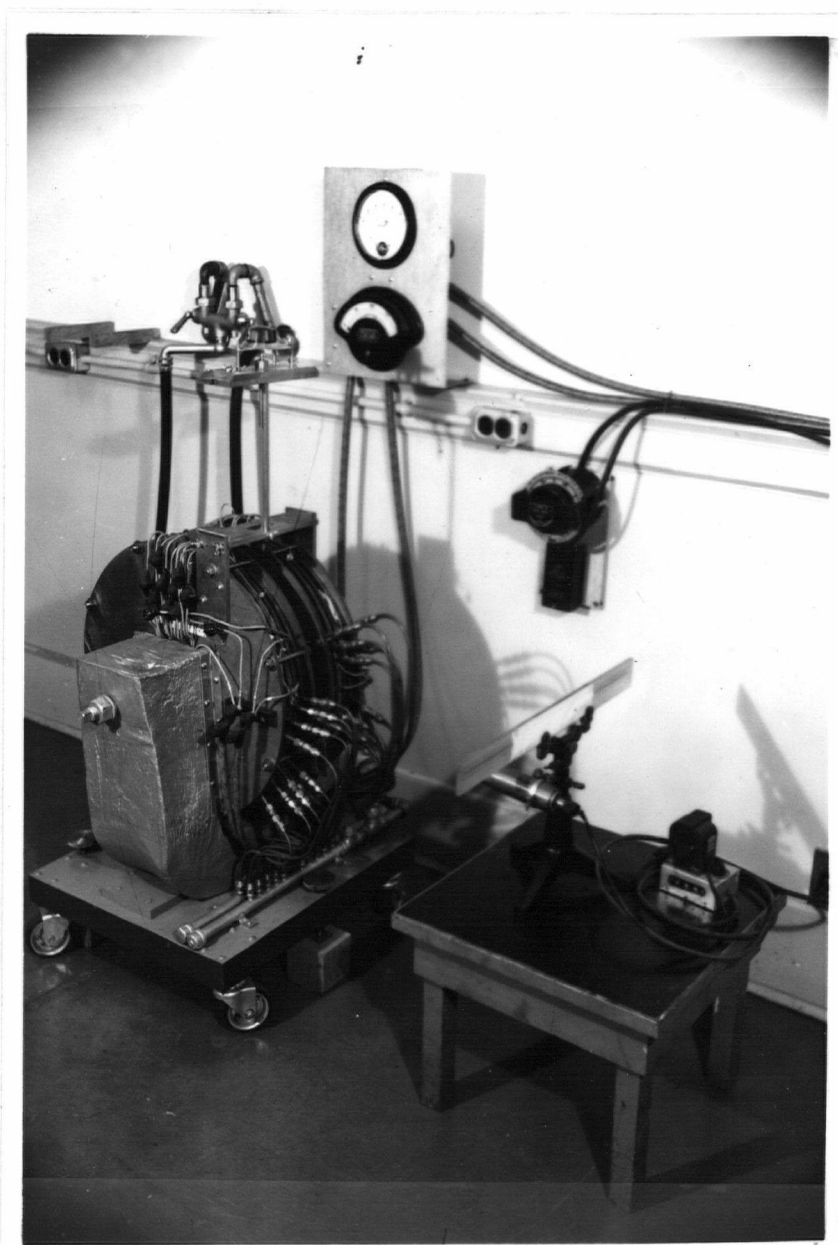


Figure 5. The completed magnet with the sample holder raised for loading.

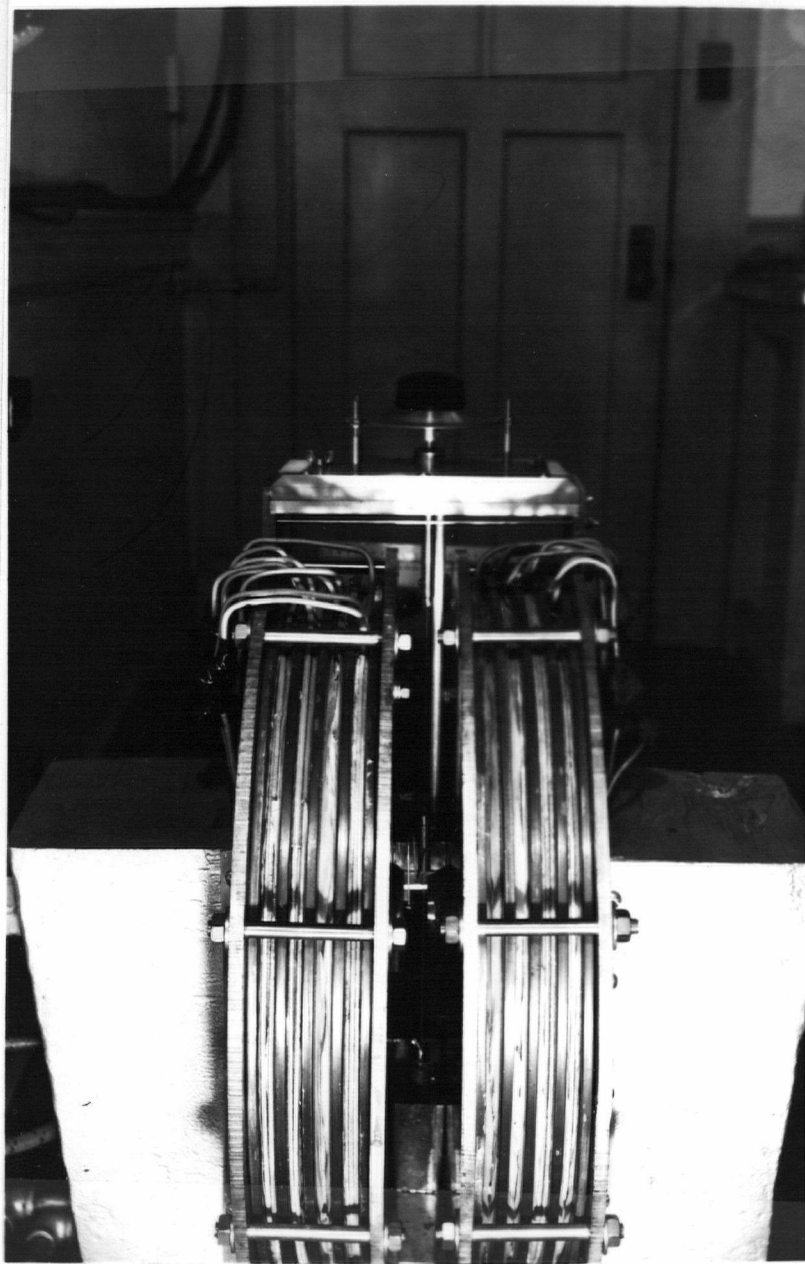


Figure 6. The completed magnet with the sample holder lowered into position for making measurements.

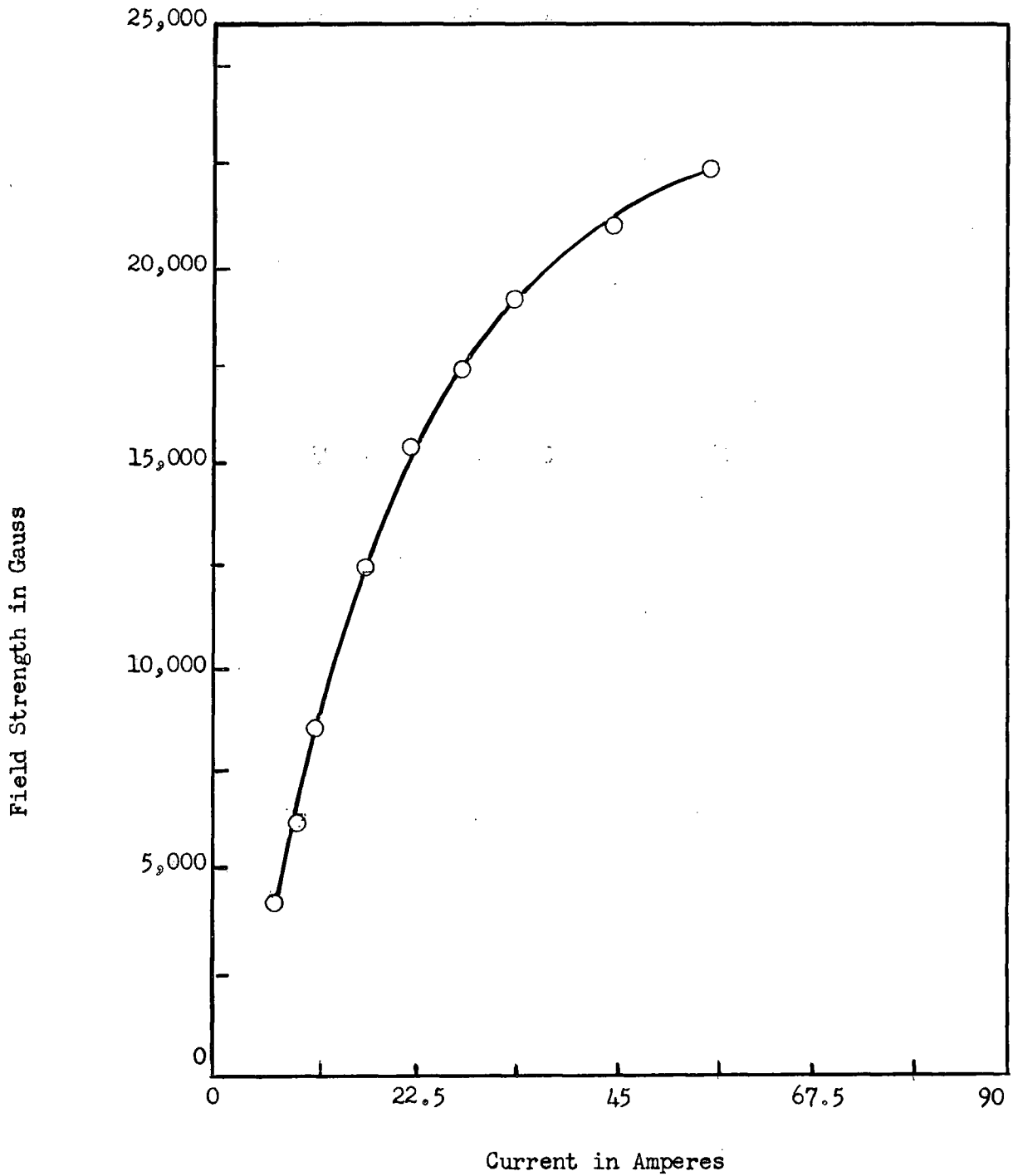


Figure 7. The field intensity in the gap of the magnet, using plane pole piece caps, for varying current. The current indicated is that measured in any one turn.

PART 2.

AN INVESTIGATION OF THE MANGANESE-RICH FERROMAGNETIC
 ALLOY OF APPROXIMATE COMPOSITION $\text{Mn}_{60}\text{Al}_{20}\text{C}_{20}$.

INTRODUCTION.

Langevin was the first to give an electron theory of paramagnetism which still forms a valuable introduction to its study.

He was able to show that for weak fields and high temperatures the susceptibility of a paramagnetic gas is given by

$$X_M = \frac{M}{H} = \frac{C}{T} \quad \text{..... 1}$$

where X_M is the susceptibility, T is the absolute temperature and C is a constant for the material concerned.

On the whole, paramagnetic susceptibilities tend to follow a modified form of equation 1, known as the Curie Weiss law. This may be written as

$$X = \frac{C}{T - \Theta}, \quad \text{or}$$

$$M = \frac{CH}{T - \Theta} \quad \text{..... 2}$$

where Θ is a characteristic constant of the substance considered.

Weiss⁹ pointed out the significance of Θ in equation 2: it means that the material behaves magnetically as if there were an additional field NM aiding the true field H . If we replace Θ by NM in equation 2 we get

$$M = \frac{C(H + NM)}{T} \quad \text{..... 3}$$

The quantity represented by NM is called the molecular field, and N is the molecular field constant. It is interpreted as supposing that the elementary magnet does have an influence on its neighbors, contrary to the assumptions of the simple Langevin theory.

From the assumption of the existence of a molecular field, Weiss was able to show that below a given temperature, the magnetic moment of a ferromagnetic substance has a definite value even when no field is applied. It can be shown that the molecular field is some thousands of times as great as the field which can arise from forces of purely magnetic origin. It was concluded therefore, that the molecular field must be electrostatic in nature.

The modern explanation of the large value of N was provided by Heisenberg^{x)}, who discovered what are known as the interchange interaction forces, or exchange forces of electrons in atoms. These forces depend upon the alignment of the electron spins in the atoms of ferromagnetics although the forces between the spins themselves are not responsible for N .

In the quantum mechanical expression for the total energy of a system of nuclei and their associated electrons, a term arises which is called the exchange integral. It takes into account the possibility that the electrons of adjacent nuclei may exchange places in the system. For the simple case of two hydrogen atoms, the integral has the form

$$J_0 = 1/2 \iint \psi_k^1 \psi_k^2 \psi_l^1 \psi_l^2 \left[\frac{2e^2}{r_{kl}} + \frac{2e^2}{r_{l2}} - \frac{e^2}{r_{lk}} - \frac{e^2}{r_{l1}} - \frac{e^2}{r_{2k}} - \frac{e^2}{r_{2l}} \right] d\tau_k d\tau_l \dots 4$$

x)

The existence of the exchange interaction was discovered independently by Dirac. Since the Dirac paper is in English, it is given here as a reference: P. Dirac; Proc. Roy. Soc.

where k, l refer to the two electrons, and $1, 2$, to the two nuclei. The ψ 's are the wave functions of the unperturbed systems (i.e. no interaction between electrons) and the \mathcal{C} 's elements of the configuration space of the specified electrons.

Heisenberg related the exchange interaction to the molecular field constant by

$$N \propto zJ \quad \dots\dots 5$$

where z = co-ordination number of the lattice.

It is seen that for ferromagnetism to occur N , and consequently J must be positive. In general, J is negative. Equation 4 shows that if J is to be positive, the term involving r_{kl} must be relatively large. The necessary conditions are found to be that the ratio of the interatomic distance to the effective mean radius of the electron density distribution of the electrons involved in the interaction shall be large, and also that the orbital quantum number for these electrons shall not be too small. There is the further basic condition that the atoms must contain incomplete groups of electrons.

Slater¹⁰ has shown that these conditions are fulfilled in the ferromagnetic metals Fe, Co, and Ni, and in some of the rare earths. He gives the following data for the ratio of interatomic distance to the mean radius of the unfilled shell, and concludes that for

TABLE 2.

Metal	Fe	Co	Ni	Cr	Mn	Gd
D/r	3.26	3.64	3.94	2.60	2.94	3.1

ferromagnetism to exist, D/r must be greater than 3.0 but not much greater.

This raises the interesting point that atoms with uncompensated electron spins which do not in the pure state exhibit ferromagnetism because the value of D/r is not suitable may combine with other non-ferromagnetic elements to form crystals whose lattice constant or distance between neighboring atoms permits a suitable value of D/r , and thus give a ferromagnetic compound.

For example, metallic manganese which exhibits a paramagnetism more or less independent of temperature has a lattice constant of 2.58 \AA whereas MnAs and MnSb with 2.85 and 2.89 \AA respectively, are ferromagnetic.

The structure sensitivity of ferromagnetism in Mn alloys requires that a careful determination of the interatomic distances between Mn atoms be made. In a ternary alloy system it becomes imperative that a degree of order be attained by the atoms if the measurement of the magnetic moment of the Mn atoms is to have any significance. A random array of atoms in the crystal lattice would result in some of the Mn atoms having the ferromagnetic condition fulfilled and others not, thereby masking the true effective moment.

It was proposed to determine the crystal structure and degree of order of the ternary system Mn-Al-C, by X-ray methods, and to measure the effective moment of the manganese atoms, using the new electromagnet.

PREVIOUS WORK.

A survey of experimental investigations of ferromagnetic manganese alloys has been given by Bozorth¹¹.

Of the ternary alloys, one of the earliest and most important systems reported was the Heusler alloy of composition Cu_2MnAl . In this, and most other ternarys, the atomic percentage of Mn is not large.

Recently a group under the supervision of E.R. Morgan¹², has made a survey of manganese-rich ferromagnetic alloys. These alloys are based on an interstitial solution of carbon in manganese. In each of the systems investigated, the ferromagnetic phase was reported having a face-centered cubic structure. Preliminary magnetic measurements, made on the Schnay magnetic balance indicated that the effective magnetic moment of the manganese atoms in the alloys was at least 1.0 Bohr magneton per atom.

One of the systems investigated in the survey was Mn-Al-C. Morgan suggested that these alloys were based on the composition Mn_3AlC which in turn, was assumed to be a stabilized form of a high temperature face-centered cubic phase of Mn_4C .

PROCEDURE.

The compositions of the materials used in making up the alloy are listed in appendix II.

In order to avoid contamination of the alloy by nitrogen or hydrogen, the melting was done under an atmosphere of purified argon in a high frequency vacuum melting unit³ designed and built in the department.

The manganese and carbon were placed in an R 84 Norton Alundum crucible. The aluminum was suspended in the furnace above the crucible by a light thread, and added to the manganese and carbon after the latter had been melted. The furnace was evacuated and the material heated for degassing. Argon was admitted after the vacuum had been restored following the degassing. The manganese and carbon were melted, and the aluminum added by raising the crucible up to the aluminum slug.

This procedure was adopted as the most successful way of obtaining a clean melt.

The alloy was chill cast into a cold brass mold.

A metallographic examination of a sample of the chill cast alloy showed evidence of segregation. This was removed by homogenizing the alloys. Heat treatments were carried out in a standard quartz tube furnace, with a sixteen inch heating element. Purified argon was passed continuously through the furnace during the annealing. The annealed samples were found to have a thick layer of green crystals form on them, in spite of the fact that the furnace had been initially evacuated, and the heating carried out in an argon atmosphere. The crystals were identified by

their X-ray pattern as MnO .

It was assumed that oxygen was entering with the argon. An attempt to prevent the formation of the oxide was made by placing the samples in a small quartz tube and evacuating and sealing the tube. The tube was placed in the furnace, and the annealing continued as before. This prevented further formation of MnO ; however, the high vapor pressure of both Mn and Al resulted in the loss of these two constituents to the walls of the tube. Finally, by placing small pieces of manganese and aluminum in the tube with the sample, the losses were reduced. In this case, however, the pure Mn and Al condensed on the samples. It was decided to fill as much of the tube as possible with the alloy, in the hope that the vapour pressures of the manganese and aluminum would reach equilibrium with negligible loss to the tube walls. Subsequent analysis for the Mn and carbon content of the samples indicated that the latter method was successful.

Debye-Scherrer powder patterns were taken of all samples, using Fe radiation and a Mn filter.

The cell parameters were calculated for all samples. Intensity measurements of all visible lines were made using a Phillips goniometer, a geiger tube and a scalar. Each line was scanned from 20 - 30 times to provide a statistical average of the counts. Background corrections were made by measuring the background count on both sides of the lines.

Intensity calculations were made for three assumed structures, and compared to the experimental values.

To check that the correct unit cell had been chosen, the density was calculated using the atomic weights and measured parameters. The results

checked with the measured density, within the experimental error of the density measurement.

Magnetic measurements were carried out for all samples at 293°K, 200°K, and 70°K, using the new electromagnet and torsion balance. Results were compared to a standard sample of nickel, and the effective moment per manganese atom was calculated, assuming a value of 0.61 Bohr magnetons for the standard nickel.

Since the demagnetizing effect is proportional to M , the magnetic moment per unit volume, and since M decreases rapidly near the Curie temperature, it was assumed that the Schnay magnet was capable of saturating the samples near the Curie temperature. Therefore the Schnay magnetic balance was used in the Curie point determinations. The samples were heated in a small furnace, in the field of the magnet. Temperatures were measured using a Chromel-Alumel thermocouple. The readings were taken as the samples cooled, and the Curie temperatures determined by extrapolating to zero magnetic moment on a plot of temperature against M .

Manganese assays were done in the department by Mr. R. Butters. Carbon analyses were done by the Vancouver Steel Co., and checked in the department by Mr. M. Swanson.

RESULTS.

The various heat treatments of the samples are shown in Table 4.

TABLE 4.

Sample No.	Heat Treatment					
(1)	Chill cast.					
(2)	Homogenized at 1100°C for 100 hr. Slow Cooled.					
(3)	??	??	??	??	??	Water Quenched.
(4)	??	??	??	??	408	?? Slow Cooled.
(5)	??	??	??	??	216	??
	Annealed	??	800°C	??	48	??
	??	??	650°C	??	24	??
	??	??	480°C	??	48	??
	??	??	200°C	??	48	??

The results of the manganese and carbon analyses are shown in Table 5. The weight per cent of aluminum was determined as (100% - Mn - C), since the presence of the manganese made it difficult to determine the amount of aluminum by chemical means.

TABLE 5.

Sample	Wt. % Mn	Wt. % C.	Wt. % Al
$\text{Mn}_6\text{OAl}_{20}\text{C}_{20}$	80.87	5.89	13.24
1	82.00	5.90	12.10
2	80.90	5.90	13.20
3	80.00	6.20	13.80
4	82.30	6.21	11.49
5	81.00	2.09	16.91

Table 6 gives the measured lattice parameter, Curie temperature, and the effective magnetic moment per manganese atom, extrapolated to zero degrees Kelvin. The moment is given in terms of Bohr magnetons. One Bohr magneton is the dipole moment associated with the spin of one electron.

The values of the lattice parameter were obtained by assuming a cubic perovskite structure. Corrections were made according to the methods described by Henry, Lipson and Wooster¹³.

The calculated and measured intensities of the X-ray lines are compared in Table 7. In presenting the relative values of intensities it was thought that the adopted method of using ratios of the different lines, as shown, was a more reliable comparison than one in which all intensities are compared to one arbitrarily chosen line, say the line with the lowest intensity is assumed to be unity. In the latter case, if the experimental value of the line chosen as a standard should be incorrect, it would tend to spoil the values of the other lines.

Table 7 shows only the calculated values assuming atoms in the

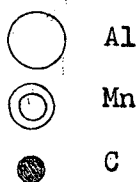
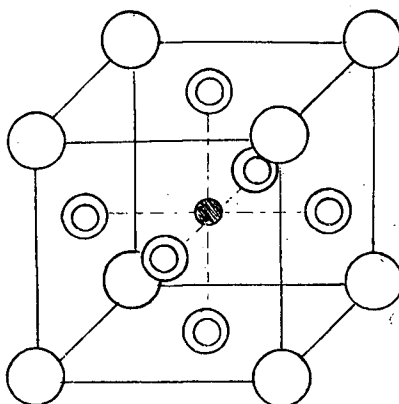
unit cell occupied the following positions:

Al 000

C $\frac{1}{2}\frac{1}{2}\frac{1}{2}$

Mn $\frac{1}{2}\frac{1}{2}0$, $\frac{1}{2}0\frac{1}{2}$, $0\frac{1}{2}\frac{1}{2}$

This structure is known as the perovskite structure, and accounts for all the lines seen on the X-ray films. Calculations for the structure having the positions of Al and C reversed give very poor agreement with experimental values. The method of calculation, and significance of the results will be described more fully under the heading of Discussion.



Assumed perovskite structure.

TABLE 6.

Sample No.	a. in Å°	Effective magnetic moment in Bohr magnetons	Curie Temp.
1	3.865	1.20 Bohr mag.	127 °C
2	3.873	0.99 "	57
3	3.873	1.08 "	57
4	3.874	1.12 "	55.5
5	3.870	1.03 "	104.0

TABLE 7.

Ratio of lines	Calculated	Measured
111:100	5.90	6.00
111:200	1.70	1.82
111:220	3.28	3.34
111:222	6.95	6.55
111:311	3.00	2.87
200:100	3.46	3.30
200:220	1.93	1.84
200:222	4.10	3.60
200:311	1.80	1.56
220:100	1.79	1.79
220:222	2.12	1.95
311:220	1.07	1.18
100:222	1.17	1.09

If maximum order is to be produced by a heat treating process, it is convenient to know the critical ordering temperature of the alloy.

According to Sykes and Jones¹⁴, the required annealing time can be greatly reduced by annealing the sample just below the critical order-disorder temperature to obtain the equilibrium degree of order at that temperature.

Continued annealing at a lower temperature will then produce the degree of order desired.

An attempt to determine the critical ordering temperature by plotting the electrical resistivity against temperature, was carried out, using a Kelvin Double bridge to measure the resistance changes. The critical temperature can be found from the discontinuity in electrical resistivity¹⁵. A photograph of the apparatus is shown in Figure 8, Plate VIII.

In this way it was hoped that a systematic heat-treating routine could be devised.

Unfortunately, the results were not reliable. The samples were obtainable in short lengths only, due to their brittleness. Changes in resistance due to end effects and the development of cracks in the specimen as it was heated were sufficient to invalidate the results.

Fortunately, as described on pages 37 - 41, a remarkable degree of order existed even in the chill cast sample.

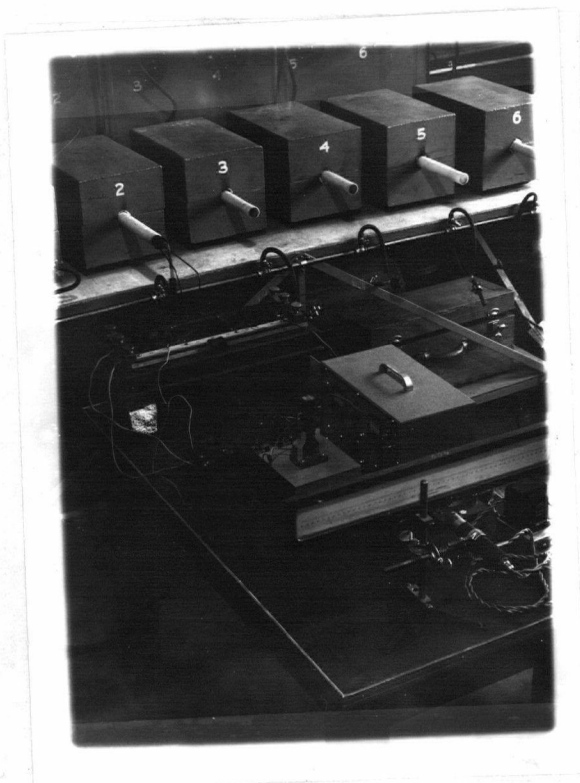


Figure 8. The apparatus used in making the resistance versus temperature measurements.

DISCUSSION AND CONCLUSIONS.

Under certain circumstances, it is possible to determine the degree of order in a crystal lattice by means of X-ray intensity measurements. The term that dominates the intensity calculation is the so-called structure factor. This term is directly dependent upon the geometrical array of atoms or molecules in the lattice. In general, the structure factor may be written as

$$F = \left[\sum_i f_i \cos 2\pi(hu_i + kv_i + lw_i) \right]^2 + \left[\sum_i f_i \sin 2\pi(hu_i + kv_i + lw_i) \right]^2$$

where f_i is the atomic scattering factor of the atom at position (U_i, V_i, W_i) in the unit cell, and h, k, l are the Miller indices for the plane concerned.

Consider the alloy Cu_3Au , which forms a face-centered cubic lattice. In the completely disordered state the atoms are distributed at random among the lattice sites and the effective atomic scattering factor is taken as the average,

$$f_{\text{au}} = 1/4 (f_{\text{Au}} + 3f_{\text{Cu}}).$$

Now because of the trigonometric terms in F , the structure factor for the planes whose indices are all even or all odd reduces to $4 \times f_{\text{au}} = f_{\text{Au}} + 3f_{\text{Cu}}$; whereas for the planes whose indices are mixed, the structure factor reduces to zero in the disordered state.

In the fully ordered lattice, the atomic scattering factor of each atom in its particular position in the unit cell is used. In this case, the structure factor for the lines corresponding to reflections from planes whose indices are homogeneous, remain unaffected, whereas the

lines corresponding to inhomogeneous indices become different from zero. Such lines are called superlattice lines, and appear only when some degree of order exists. Hence they can be used as a measure of the degree of order.

The situation is quite different for the case of the perovskite structure, however. Here the unit cell is effectively face-centered cubic, with an extra atom in the body-centered position.

Assuming first, a completely ordered structure, with atoms at the positions

Al 000

C $\frac{1}{2}\frac{1}{2}\frac{1}{2}$

Mn $\frac{1}{2}\frac{1}{2}0$, $\frac{1}{2}0\frac{1}{2}$, $0\frac{1}{2}\frac{1}{2}$,

the structure factors reduce to the terms given in column two of Table 8; the evaluated result is given in column three.

For the fully disordered lattice, $f_{av} = 1/5(f_{Al} + f_C + 3f_{Mn})$ must be used.

The structure factors are given in column four, and evaluated in column five. Since F appears as a squared term in the intensity calculation, the absolute values of F are given.

TABLE 8.

Line	F ordered	(F ord.)	F disordered	(F dis.)
100	$f_{Al} - f_{Mn} - f_C$	12.1	$1/5(f_{Al} + f_C + 3f_{Mn}) \cdot 1$	13.86
110	$f_{Al} - f_{Mn} + f_C$	2.3	" . 1	12.02
111	$f_{Al} + 3f_{Mn} - f_C$	47.80	" . 3	32.58
200	$f_{Al} + 3f_{Mn} + f_C$	50.55	" . 5	50.55
210	$f_{Al} - f_{Mn} - f_C$	5.90	" . 1	9.06
211	$f_{Al} - f_{Mn} + f_C$	> 2.3	" . 1	7.80
220	$f_{Al} + 3f_{Mn} + f_C$	36.55	" . 5	36.55
221	$f_{Al} - f_{Mn} - f_C$	> 2.3	" . 1	6.78
222	$f_{Al} + 3f_{Mn} + f_C$	28.1	" . 5	28.1
300	$f_{Al} - f_{Mn} - f_C$	> 2.3	" . 1	-
310	$f_{Al} - f_{Mn} + f_C$	> 2.3	" . 1	-
311	$f_{Al} + f_{Mn} - f_C$	26.00	" . 3	18.00

It is seen that under the assumption of complete disorder, the lines 100, 110 etc., not only remain non-zero, but actually increase over the ordered state.

Unfortunately there is no way of determining the value of the order parameter for the system under consideration, since the line intensities do not change in a linear way with the degree of order. It is interesting to note that the lines 200, 220 and 222 are unaffected by the degree of order in the lattice.

Significant information can be obtained from a consideration of line 110. In the completely ordered alloy, the intensity is seen to

be very low, whereas in the disordered state its value is comparable to that of line 100.

The experimental intensity of the 110 line was too small to measure.

Similarly, the intensity of line 211 in the ordered state is lower than that of 110, whereas in the disordered state it is close to that of line 210. Again, the intensity measurements were unable to detect 211.

It is indicated therefore, that a fairly high degree of order exists even in the chill cast sample. This conclusion, however, can only be stated from the results of the intensity measurements. To say that ordering exists because of the appearance of the 'superlattice lines', as reported by Morgan¹², is quite erroneous.

Indeed, as already pointed out, this could lead to the conclusion that the order is increasing when in reality it is decreasing, since the intensity of the 100, 110, and 211 lines increase with disorder.

The calculations of density from the considerations of the unit cell led to good agreement with the experimentally determined value.

Goldsmidt¹⁶ has shown that a criterion of the stability of the perovskite structure can be obtained from the fact that maximum stability occurs when the parameter t is equal to unity, where t is defined as:

$$t = \frac{r_{Al} + r_{Mn}}{\sqrt{2}(r_C + r_{Mn})}$$

Here r is the ionic radius. The calculated value for Mn_3AlC was 1.002.

It is interesting to note that a perovskite structure of Mn_4C , which Morgan reported as unstable leads to a value of 1.10 for t .

An examination of Table 6 reveals that the Curie temperatures decrease as the lattice parameters increase. This would indicate that the

ratio of interatomic distance to the ionic diameter of the manganese atom is somewhat too large for the maximum energy of magnetization. In the chill cast sample, the interatomic distance was 3.865 Å°. Assuming a 3d ionic radius of 0.91¹⁷ Å°, the ratio of $D/r = \frac{3.865}{0.91} = 4.24$

This also indicates, that the radius is too large for maximum exchange interaction, as seen by referring to Table 2, page 26, and confirms the conclusion drawn from the Curie temperature measurements.

It is interesting to note that the value of 1.2 Bohr magnetons per manganese atom for the chill cast alloy is in agreement with the value deduced by Pauling¹⁸ who attempted to account for the experimental values of saturation magnetization of the elements.

The experimental curve is shown in Figure 9 , Plate IX.

This, of course, makes it difficult to account for the values of saturation magnetization of the other samples, unless it is assumed that a greater degree of disorder exists, than for the chill cast specimen, resulting in fewer Mn atoms in the ferromagnetic state.

Some justification for this assumption is given by the faint appearance of line - 110 in the X-ray pattern of samples 2 and 3, as seen on Plate X. No indication of the presence of line 110 is given in the chill cast X-ray film, thereby indicating a higher degree of order in the chill cast sample.

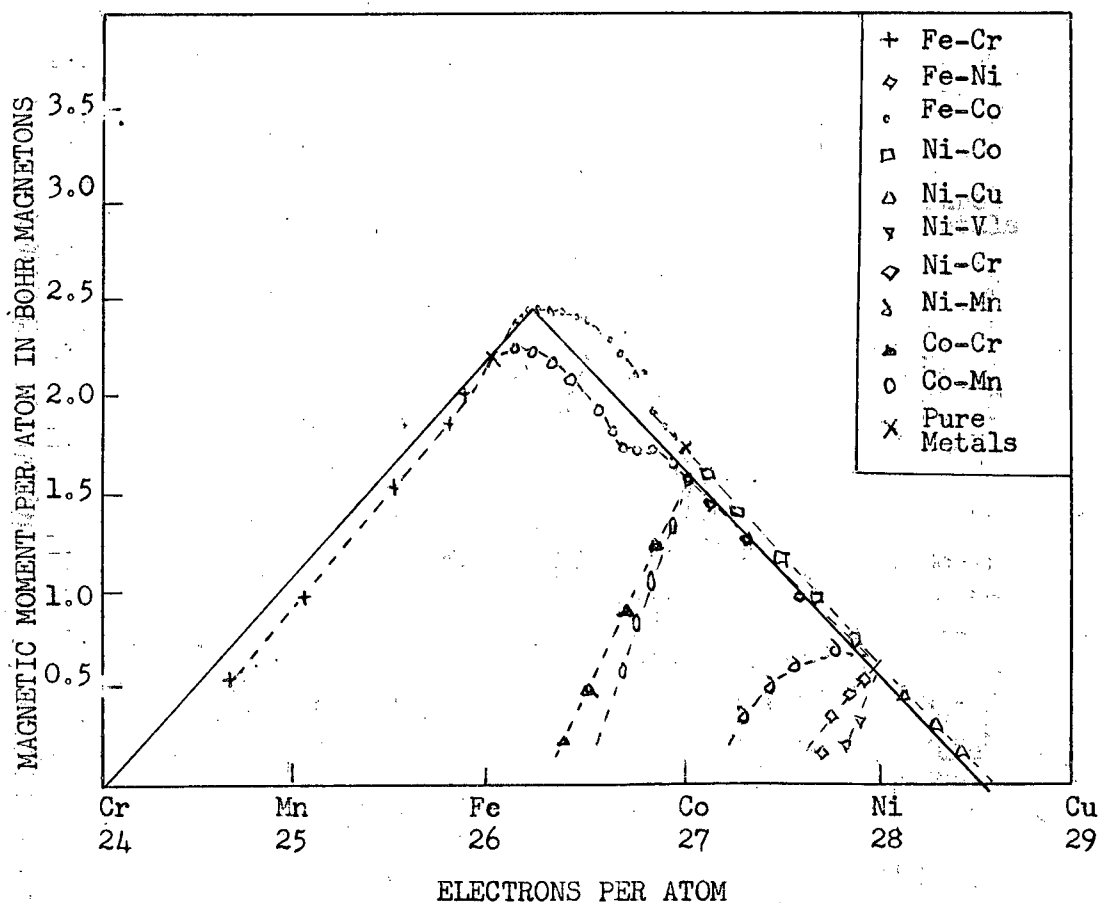


Figure 9. A plot of magnetic moment per atom against atomic number. The solid line is the theoretical value; the dotted lines show the experimental measurements.

PLATE X

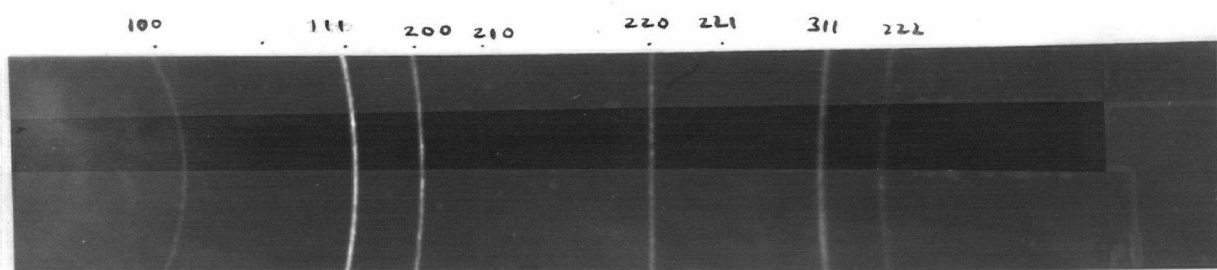


Figure 10. The Debye-Scherrer X-ray powder pattern
for sample number 1.

APPENDIX I.

Design Calculations:

1. Estimate of ampere-turns required

$$\begin{aligned}
 (NI - H_i l_i) &= H_a l_a \\
 &= 18000 \text{ gauss} \times 2.02 \frac{\text{amp-turns}}{\text{gauss-inch}} \times 1 \text{ inch.} \\
 &= 36,400 \text{ ampere turns.}
 \end{aligned}$$

From trial designs, final estimated ampere-turns = 45,000.

2. Power to be dissipated.

Assumed temperature rise = 20°C

" rate of flow of water = 50cc/sec.

$$\begin{aligned}
 \therefore \text{Power dissipation} &= 20^\circ\text{C} \times 50 \frac{\text{cc}}{\text{sec.}} \times 4.18 \frac{\text{joules}}{\text{cal}} \times 1 \frac{\text{cal}}{^\circ\text{C.cc}} \\
 &= 4180 \text{ watts.}
 \end{aligned}$$

3. Effective resistance of copper in the coils:

$$R = \frac{\text{power}}{(\text{ampere-turns})^2} = \frac{4180}{(45,000)^2} = 2.06 \times 10^{-6} \text{ ohms.}$$

4. Specific resistance of copper at 20°C is

$$\rho_o = 6.79 \times 10^{-7} \text{ ohm-inch.}$$

Temperature coefficient of resistance of copper = α

$$\therefore \text{Specific resistance at } 40^\circ\text{C} = \rho_o (1 + \alpha \Delta t)$$

$$= 6.79 \times 10^{-7} \text{ ohm inch } (1 + 3.93 \times 10^{-3} \times 20)$$

$$\text{i.e. } \rho_{40^\circ\text{C}} = 7.324 \times 10^{-7} \text{ ohm-inch.}$$

Let L = mean circumference of the coil.

A = total cross-sectional area of coil assemblies

f = space factor of the windings.

Assume $f = 3$.

$$\text{Then } R = \frac{\rho L}{A/f}$$

$$\text{i.e. } \frac{L}{A} = \frac{R}{\rho f} = \frac{2.06 \times 10^{-6}}{7.324 \times 10^{-7} \times 3} = 0.938 \quad \dots\dots 1$$

The shape of the pole piece is shown in Figure 10, Plate XI

The width of each coil assembly will be 3 inches, which provides a working space of 2 inches between the coil assemblies.

From Figure 10 we have

$$\tan \phi = \frac{3 - 1}{3\frac{1}{2}} = \frac{x}{3}$$

$$\therefore x = 1.715$$

$$\frac{A}{2} = 3b + \frac{1}{2} \times 3 \times 1.715$$

$$\therefore A = 6b + 5.15 \quad \dots\dots 2$$

$$L = \pi \left[\frac{O.D. + I.D.}{2} \right]$$

$$\begin{aligned} \text{That is } L &= \pi \left[\frac{(6 + 2b + 3/4) + (6 - 1.715 + 3/4)}{2} \right] \\ &= \pi [b + 5.89] \quad \dots\dots 3 \end{aligned}$$

From equations 1, 2 and 3, we can evaluate A, L, and b.

$$A = 38.15 \text{ square inches}$$

$$L = 35.8 \text{ inches}$$

$$b = 5.5 \text{ inches.}$$

$$\text{Area of copper} = \frac{A}{3} = \frac{38.15}{3} = 12.71 \text{ square inches.}$$

If we assume one turn of solid wire, then the copper density per ampere is

$$\begin{aligned} \frac{\text{Area of copper}}{\text{Total amperes}} &= \frac{\frac{4}{\pi} \times 10^6}{1 \text{ in}^2} \times \frac{12.71}{4.5 \times 10^4} \text{ amperes} \\ &= 360 \text{ circ. mils/ampere.} \end{aligned}$$

Assume the source voltage is 120 volts.

$$\text{Then current} = \frac{\text{Power}}{\text{volts}} = \frac{4180}{120} = 34.8 \text{ amperes.}$$

$$\therefore \text{Area of the wire} = 35 \text{ amperes} \times 360 \frac{\text{circ.mils.}}{\text{ampere}}$$

$$= 12,600 \text{ circ. mils.}$$

$$\#10 \text{ commercial wire size} = 12,535 \text{ circ.mils.} = .00984 \text{ square inch.}$$

$$\text{Number of turns required} = \frac{12.71}{.00984} = 1292.$$

$$\text{Current required} = \frac{45000}{1292} = 34.8 \text{ amperes.}$$

$$\text{Resistance of coils} = 1292 \times \frac{35.8 \text{ ft.}}{12} \times \frac{.824}{.928} \times \frac{1}{1000} \frac{\text{ohms}}{\text{ft.}}$$

$$= 3.42 \text{ ohms.}$$

Voltage required for series connections

$$= 3.42 \text{ ohms} \times 34.8 \text{ amps.} = 119.2 \text{ volts.}$$

$$\text{Power dissipated} = 34.8 \text{ amps.} \times 119.2 \text{ volts} = 4150 \text{ watts.}$$

From the diagram shown in Figure 2, Plate II, the mean path length in the iron port of the magnetic circuit is 46 inches.

To determine the value of the field in the iron, H_i , the following relation is used:

$$B_i = B_a g l$$

where

B_i = flux density in iron

B_a = flux density in air gap = 18000 gauss.

g = geometrical factor

$$= \frac{\text{area of small diameter of pole-piece}}{\text{large}}$$

$$= \frac{1}{9}$$

l = leakage factor

= $\frac{\text{total flux through largest part of pole-piece}}{\text{flux through air gap}}$

$$l = \frac{\int_0^1 2\pi r H dr + \int_1^5 2\pi r \cdot \frac{H}{r} dr}{\int_0^1 2\pi r H dr} = 9.$$

$$\therefore B_i = B_a \text{ gl} = B_a = 18000 \text{ gauss.}$$

From Roters, for $B_i = 18000$ gauss,

$$H_i = 200 \frac{\text{amp. turns}}{\text{inch.}}$$

\therefore Total ampere turns required

$$\begin{aligned} &= NI = H_i l_i + H_a l_a \\ &= 200 \times 46 + 36,400 \\ &= 45,600 \text{ ampere turns.} \end{aligned}$$

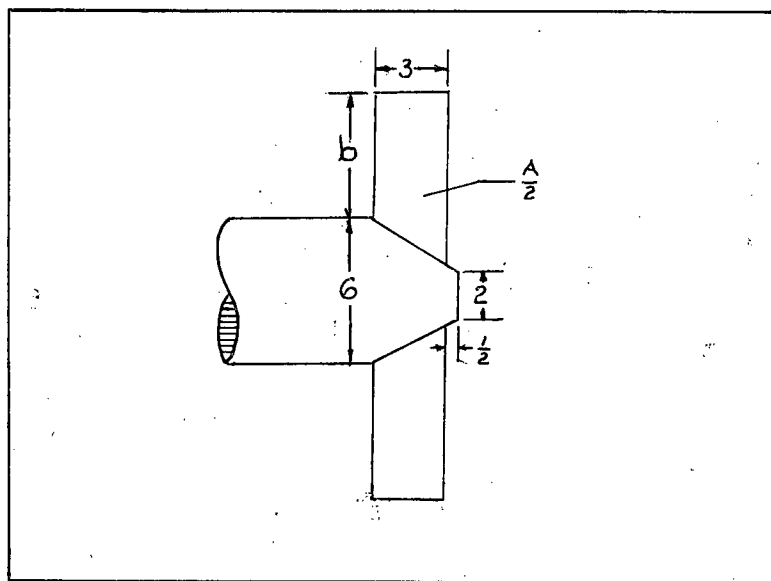


Figure 10 a. Dimensions of pole piece and coil assembly.

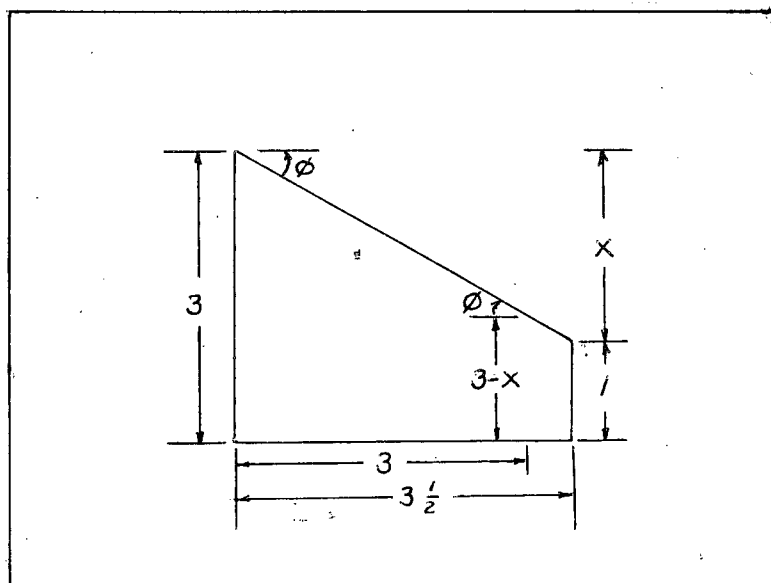


Figure 10 b. Detail of pole piece.

APPENDIX II.

The following base materials were used for the alloys:

Manganese: 99.9 percent purity, donated by the Electromanganese
Corporation of America.

Aluminum: 99.99 percent purity, donated by the Aluminum Company of
Canada.

Carbon: Spectroscopic purity.

BIBLIOGRAPHY

1. R. Buehl and J. Wulff, Rev. Sci. Inst. 9 224, (1938)
2. R. Schnay, Masters Thesis, University of British Columbia, 1951.
3. R. Piercy, " " " " " " " " 1952.
4. Ewing, 'Magnetic Induction in Iron and other Metals'.
5. W. Sucksmith, Proc. Roy. Soc., A170 551, 1939.
6. Roters, 'Electromagnetic Devices'.
7. R. Fereday, Proc. Roy. Soc., 46 214.
8. R. Shier, Thesis, University of British Columbia, 1953.
9. P. Weiss, Jour. Phys. (4), 6, 661.
10. J. Slater, Phys. Rev., 36 57, 1930.
11. R. Bozorth, 'Ferromagnetism', D. Van Nostrand Co., 1951.
12. E.R. Morgan, Progress Report.
13. Henry, Lipson and Wooster, 'Interpretation of X-ray Diffraction
Photographs,' McMillan Co. London, 1951.
14. C. Sykes and F. Jones, Proc. Roy. Soc., A166 376, 1938.
15. Kurnakov and Agnew, Jour. Inst. Metals, 46 484.
16. M. Goldschmidt, 'Geochim. Verlungsgesetze der Elemente VII, 1927.
17. J. Smithells 'Metals Reference Book' Butterworth, London, 1949.
18. L. Pauling, Phys. Rev. 54 899.